Open Research Online

Molecular line observations of IC 443 - the interaction of a molecular cloud and an interstellar shock

Journal Item

oro.open.ac.uk

Molecular line observations of IC 443. The interaction of a molecular cloud and an interstellar shock

Glenn J. White[1], Ruth Rainey[1], Saeko S. Hayashi[2], and Norio Kaifu[2]

[1] Astrophysics Group, Queen Mary College, University of London, Mile End Road, London E1 4NS, England
[2] Nobeyama Radio Observatory, Nobeyama, Minamisaku, Nagano 384-13, Japan

Summary. The supernova remnant IC 443 is colliding with several molecular clouds which are now situated close to the expanding rim. Observations of CO, ^{13}CO, HCO$^+$, and HCN at frequencies between 88 and 356 GHz have been obtained towards several of these molecular clouds to examine the effects of the strong shock with the neutral gas in the clouds. The spatial distributions of CO, HCN and HCO$^+$ are found to be very similar, and well correlated with that of shocked molecular hydrogen. The molecular lines observed from this area are very broad, having linewidths of up to 90 km s^{-1}. The effect of the shock has been to cause extensive fragmentation of the clouds into dynamically unstable systems of fragments having typical size scales of 0.1–0.3 pc. A spectral line survey between 84 and 104 GHz has been carried out, which includes a number of molecular species which have been chosen as diagnostics of shock chemistry. Modelling has been carried out for several molecular species, which shows that CO emission from the high velocity gas is usually optically thin, but for other species, the lines may be optically thick and subthermally excited.

Key words: interstellar medium: molecules – radio lines: molecular – supernova remnant: IC 443

almost unique kinematic structure, there were suggestions that the chemical abundances in the shocked gas differ from those of more "standard" dense molecular cloud cores. In particular, the OH/CO and HCO$^+$/CO abundance ratios were found to be ~ 100 and 10 times greater in IC 443 than for other molecular clouds. Other abundance ratio estimates for HCN/CO and CS/CO and upper limits on SiO and SO similarly indicated no significant abundance enhancements for those species (see DeNoyer, and Frerking, 1981; and DeNoyer, 1983 for fuller discussion). These variations of abundance ratio relative to other galactic molecular clouds could result as a consequence of shock chemistry processing, where the elevated temperatures and effects of dissociation occurring during the passage of a strong shock can lead to the anomalous relative abundances reported in a number of the molecular species. Recently, maps have become available of the distribution of shocked molecular hydrogen (Burton et al., 1985), and far-IR continuum radiation from IRAS (Cudlip, Braun; private communications). To improve our understanding of the astrophysical and chemical processes occurring in this object, we have mapped several of the regions containing shocked gas in IC 443, using the Nobeyama 45 m, Kitt Peak 12 m, and UKIRT 3.8 m telescopes at millimetre and submillimetre wavelengths, in a variety of molecular lines.

1. Introduction

A section of the shell of the supernova remnant IC 443 is expanding into a nearby molecular cloud. Evidence for interaction between the two has been presented in a series of papers (DeNoyer, 1978, 1979; Treffers, 1979; Fesen and Kirshner, 1980; Dickinson et al., 1980; DeNoyer and Frerking, 1981 and Huang et al., 1986). Excitation of the molecular gas by the expanding supernova shell is indicated by the presence of extremely broad spectral linewidths of at least 30–40 km s^{-1}, which have been observed in the HI, OH, CO, CS, HCN and HCO$^+$ lines towards a number of positions lying close to the edge of the shell. These broad lines are excited as a result of interaction with a shock front at the edge of the supernova remnant. In addition to the

2. The observations

The observations reported in this paper were obtained using the Nobeyama 45 m telescope in the 80–115 GHz range, the Kitt Peak 12 m telescope at 220 and 230 GHz, and the United Kingdom Infrared Telescope (UKIRT) at 345 and 356 GHz. The data were collected during April 1985 and 1986 (Nobeyama), May 1985 (Kitt Peak) and August 1983 and 1985 (UKIRT). All the data have been calibrated to a scale of main beam brightness temperature T_r, where we have estimated the product of the forward spillover efficiency, η_{fss}, and the beam coupling onto a uniform source of the same as size as the diffraction limited beam, η_c, to be 0.4 (90 GHz), 0.27 (115 GHz), 0.48 (230 GHz) and 0.45 (345 GHz). We have adopted this calibration scale in order to compare data from the different telescopes.

At Nobeyama, mapping observations were carried out simultaneously in the CO, HCO$^+$ and HCN J = 1 − 0 lines, and in some cases the CS J = 2 − 1 line, using a polarization splitter to send

---

338

orthogonal polarizations into two different receivers operating in the appropriate frequency bands. The spectra were then processed using a 2 GHz bandwidth ADS back-end. At Kitt Peak, both orthogonal polarizations were observed simultaneously, using a filter bank backend, and were then coadded. At UKIRT, a single polarization was observed using the QMC submillimetre heterodyne receiver (White et al., 1981; White et al., 1986). The single sideband equivalent noise temperatures (including atmospheric emission and telescope losses) were typically 700–1000 K (Nobeyama), 2000–3000 K (Kitt Peak) and 350 K (UKIRT). The beam sizes of the telescopes were 20″, 15″, 30″ and 55″ at 88, 115, 230 and 345 GHz respectively. All observations were regularly calibrated for atmospheric absorption using standard chopper calibration and sky-tip measurements.

3. The results

3.1. CO, HCO⁺ and HCN observations

The CO $J=1-0$ distribution was mapped at Nobeyama, mostly on a 15″ sampling grid. The nominal $(0,0)$ position was chosen as RA (1950) = $+06^h14^m43^s0$, DEC (1950) = $+22°23'00''$. This was selected as it is the position from which molecular hydrogen emission was initially detected (Treffers, 1979), and lies 33″ from the coordinates of the high velocity emitting region IC 443C, reported by DeNoyer (1979). One hundred and fifty positions were observed, mostly covering areas where high velocity gas was found to be present, and with reference to the molecular hydrogen and IRAS 60 μm maps. In Fig. 1 we show an example of the spectra obtained.
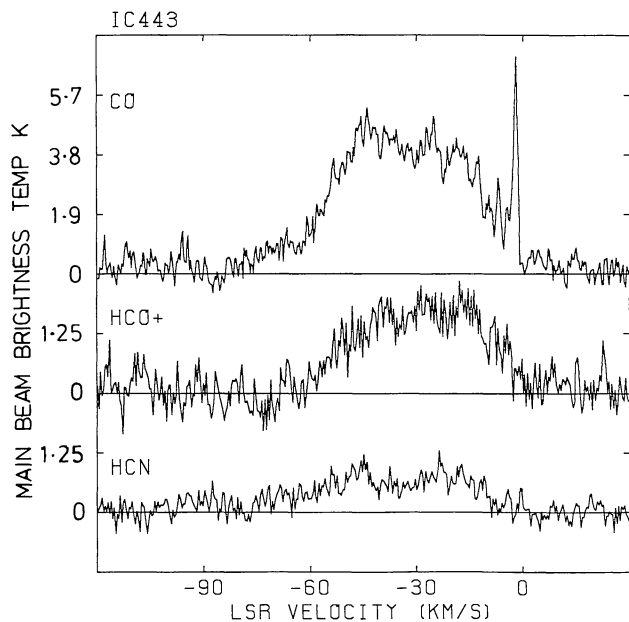

Fig. 1. Spectra obtained towards the position RA (1950) = $06^h14^m38^s9$, DEC (1950) = $+22°22'45''$, showing the high velocity gas in the $J=1-0$ lines of CO, HCO⁺ and HCN. The temperature scale up the vertical axis for this and subsequent diagrams is in units of main beam brightness temperature unless otherwise stated

The CO $J=1-0$ spectrum shows emission from a narrow spectral component at a velocity of -3 km s⁻¹, but is dominated by a broad emission line extending over a total linewidth of 80 km s⁻¹, and having a half-power linewidth of 47 km s⁻¹. The narrow emission lines are characteristic of the ambient cloud material which is widespread in the direction of IC 443 (Cornett et al., 1977). The broad line emitting regions are more localised, and are closely correlated with the position of the edge of the supernova remnant. The broad CO line is non-gaussian in shape, and, as will be seen later, is almost certainly a blend of the emission from several different cloud fragments. Profiles are also shown in Fig. 1 of the HCO⁺ and HCN $J=1-0$ transitions, which were observed *simultaneously* with the CO spectrum. Both molecular species have the same broad lineshape as seen in the CO spectrum, although the narrow feature corresponding to gas at the ambient cloud velocity is not present. The HCO⁺ and HCN intensities integrated over the line profile (correcting for the telescope efficiency at the respective frequencies) are factors of 2.6 and 5.3 respectively less than that of the CO $J=1-0$ spectrum. This is a quite remarkable result at first sight, considering that the high velocity CO emission is believed to be optically thin at the nearby IC 443C position (DeNoyer, 1979). The high velocity gas is widespread over the area mapped, although positions which exhibit gas having velocities extending more than 40 km s⁻¹ from the ambient cloud are rare. In Fig. 2 we show a selection of spectra at several different positions. It can be seen that both the line intensity and lineshape vary rapidly from position to position, indicating a complex geometry for the region. In some cases, the HCO⁺ linewidth is greater than that of CO.

In Fig. 3, maps are shown of the CO $J=1-0$ distribution near the edge of the expanding supernova shell. The maps have been obtained by integrating across the spectra in 10 km s⁻¹ wide velocity intervals. At the most negative velocities, the CO distribution is dominated by emission from a single region of the cloud with a deconvolved diameter of 20″, centred at RA (1950) = $06^h14^m41^s9$, DEC (1950) = $+22°22'40''$. This high velocity cloud fragment has a circular structure, which becomes more asymmetric as the velocity becomes more positive. In all, at least seven distinct cloud fragments can be discerned in the maps shown in Fig. 3, and it is likely that the individual spectra observed towards many of the positions, are blends of the emission from several of the fragments along particular lines of sight. The large-scale structure of the CO distribution is that of an elongated ridge lying in a NE-SW direction, with a similar orientation to that of the edge of the supernova remnant shell. The detection of the high velocity gas and its spatial distribution confirms the association between the supernova shell and the excitation of the neutral material in the cloud to be certain.

In Fig. 4, the integrated distributions of the HCO⁺ and HCN $J=1-0$ transitions are shown for the same area as Fig. 3. The spatial distribution of these molecules exhibit an almost identical spatial distribution to the CO (and are also very similar to that of molecular hydrogen), although in HCO⁺ and HCN the peak positions are slightly NE of the highest velocity CO peak. The similarity of the spatial distributions suggest that the three molecular species may have a common excitation mechanism, and are emitted from the same volume of gas.

In Fig. 5, maps of integrated CO $J=1-0$ emission are shown for three other areas in the IC 443 cloud where high velocity emission was detected (although for these cases, the linewidth $\Delta v \leq 20$ km s⁻¹), none of these positions having evidence for the
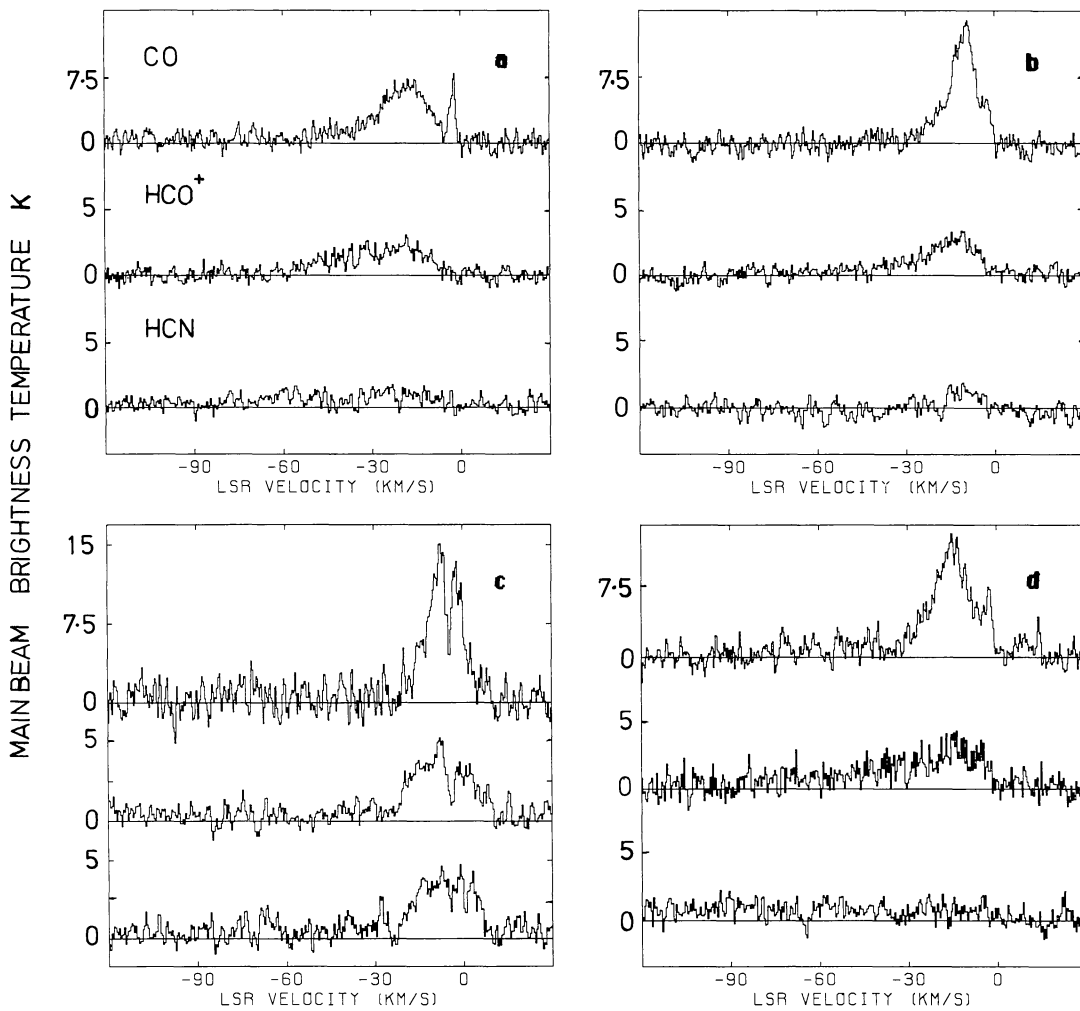
Fig. 2a–d. Spectra obtained towards several other positions in the IC 443 complex. The vertical scale is in units of main beam brightness temperature (K). The spectra were obtained towards the positions (1950 coordinates RA, DEC): **a** 06^{h}14^{m}43^{s}0, +22°23'15''; **b** 06^{h}14^{m}51^{s}1, +22°23'45''; **c** 06^{h}13^{m}42^{s}0, +22°33'40''; **d** 06^{h}14^{m}44^{s}1, +22°23'30''

very high velocity emission detected from the cloud fragment near RA (1950) = 06^{h}14^{m}41^{s}9, DEC (1950) = +22°22'40''.

In addition to the CO J = 1 − 0 data, we have obtained spectra at 27 positions in the CO J = 2 − 1 transition. In Fig. 6 a selection of CO J = 2 − 1 spectra observed at similar positions to the J = 1 − 0 data are shown. The same trends in linewidth and spatial structure are clearly seen, although the emission at the velocity corresponding to the *ambient* gas is considerably weaker than observed in the J = 1 − 0 transition.

Observations of the J = 2 − 1 transition of ^{13}CO were obtained at two positions in the shocked gas. In Fig. 7a we show an overlay of CO and ^{13}CO J = 2 − 1 measurements at the position RA (1950) = 06^{h}13^{m}42^{s}0, DEC (1950) = +22°33'40''.

This position, which contains the strongest *peak* intensity for the shocked gas observed anywhere in the IC 443 complex, was selected on the basis of the IRAS 60 μm map (Cudlip, private communication), which shows a local peak at these coordinates. The CO J = 2 − 1 spectrum has a full width of 30 km s^{-1}, and a narrow dip at −5 km s^{-1}. We have mapped around this position in both the CO J = 1 − 0 and 2 − 1 lines, and find that for several positions which contain no evidence for shocked gas,

a weak, narrow, emission line is observed at a velocity of −5 km s^{-1}. We therefore conclude that the dip in the CO spectra arises from the presence of cool foreground material along the line of sight. A similar dip is seen in the CO and HCO$^+$ J = 1 − 0 spectra, but not in the HCN line. In Fig. 7b, we show an HCO$^+$ J = 4 − 3 spectrum obtained at UKIRT, which shows a strong emission feature at a similar velocity to that of ^{13}CO. The ^{13}CO spectrum shown in Fig. 7a contains emission at similar velocities in the shocked gas seen in the CO line, as well as a narrow ^{13}CO *emission* line, which is at the same velocity as the dip in the CO spectrum. During April 1986 we reobserved this area in the J = 1 − 0 HCN, HCO$^+$ and J = 2 − 1 CS lines. The high velocity emitting region is clearly resolved as can be seen in Fig. 5, in HCN and HCO$^+$, but appeared unresolved in the CS line, for which we measured a peak main beam brightness temperature of 2 K. The average antenna temperature ratio of the CO/^{13}CO main beam brightness temperatures in the J = 2 − 1 transition over the velocity range −7 to −18 km s^{-1}, is 39.

A ^{13}CO spectrum obtained close to the high velocity fragment at RA (1950) = 06^{h}14^{m}41^{s}9, DEC (1950) = +22°22'40'', shows no emission at velocities corresponding to that of the
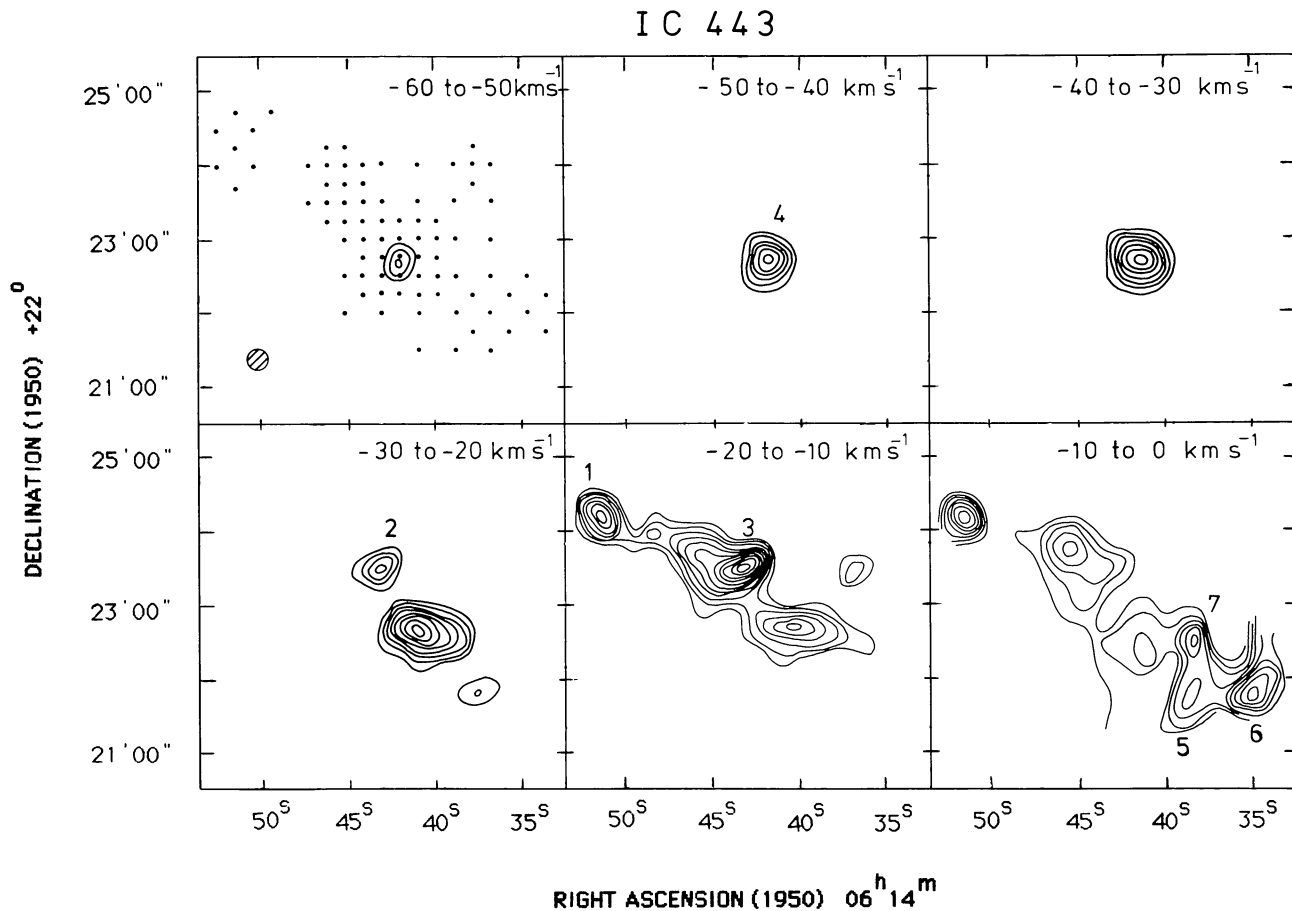
IC 443

Fig. 3. Maps of the distribution of CO $J=1-0$ emission integrated in $10\,\mathrm{K\,km\,s^{-1}}$ intervals along the SE edge of the supernova remnant shell. The contours are in units of main beam brightness temperature $\mathrm{K\,km\,s^{-1}}$, the lowest contour level being $15\,\mathrm{K\,km\,s^{-1}}$, and successive contours being spaced at $3.7\,\mathrm{K\,km\,s^{-1}}$ intervals

shocked gas, and we can set a lower limit of 31 on the ratio of peak intensities of $CO/^{13}CO$. This limit is somewhat worse than that which has been determined for the $J=1-0$ transition at a nearby position (DeNoyer and Frerking, 1981) of 62.

CO $J=3-2$ spectra were obtained towards the positions designated IC 443B and IC 443C by DeNoyer (1979). These spectra are shown in Fig. 8. We note that the peak intensity of the $J=3-2$ line is about twice that of the $J=1-0$ transition for
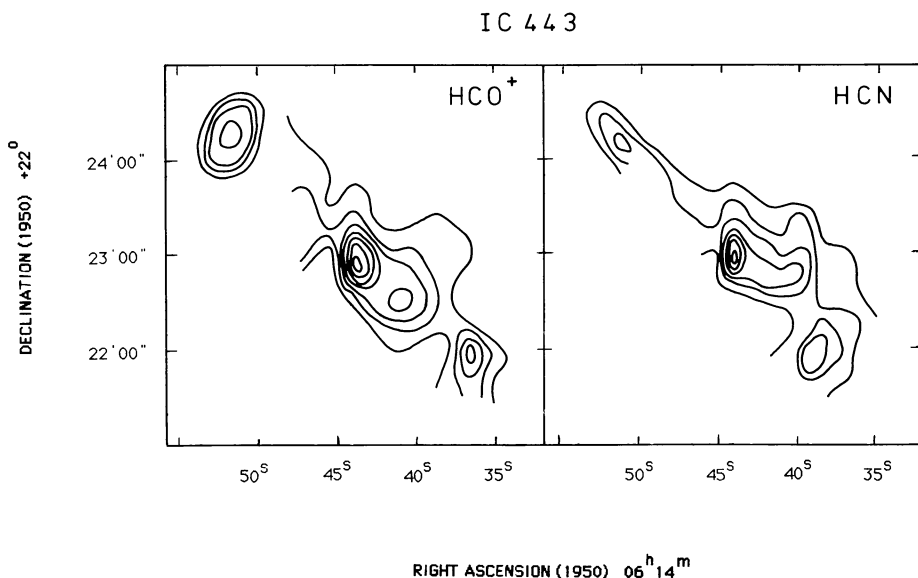
IC 443

Fig. 4. Maps of the distribution of HCO^+ and HCN $J=1-0$ emission integrated over the velocity interval -90 to $0\,\mathrm{km\,s^{-1}}$ for the same area as shown in Fig. 3. The contours are in units of main beam brightness temperature, the lowest being $25\,\mathrm{K\,km\,s^{-1}}$, and the spacing between levels being $25\,\mathrm{K\,km\,s^{-1}}$
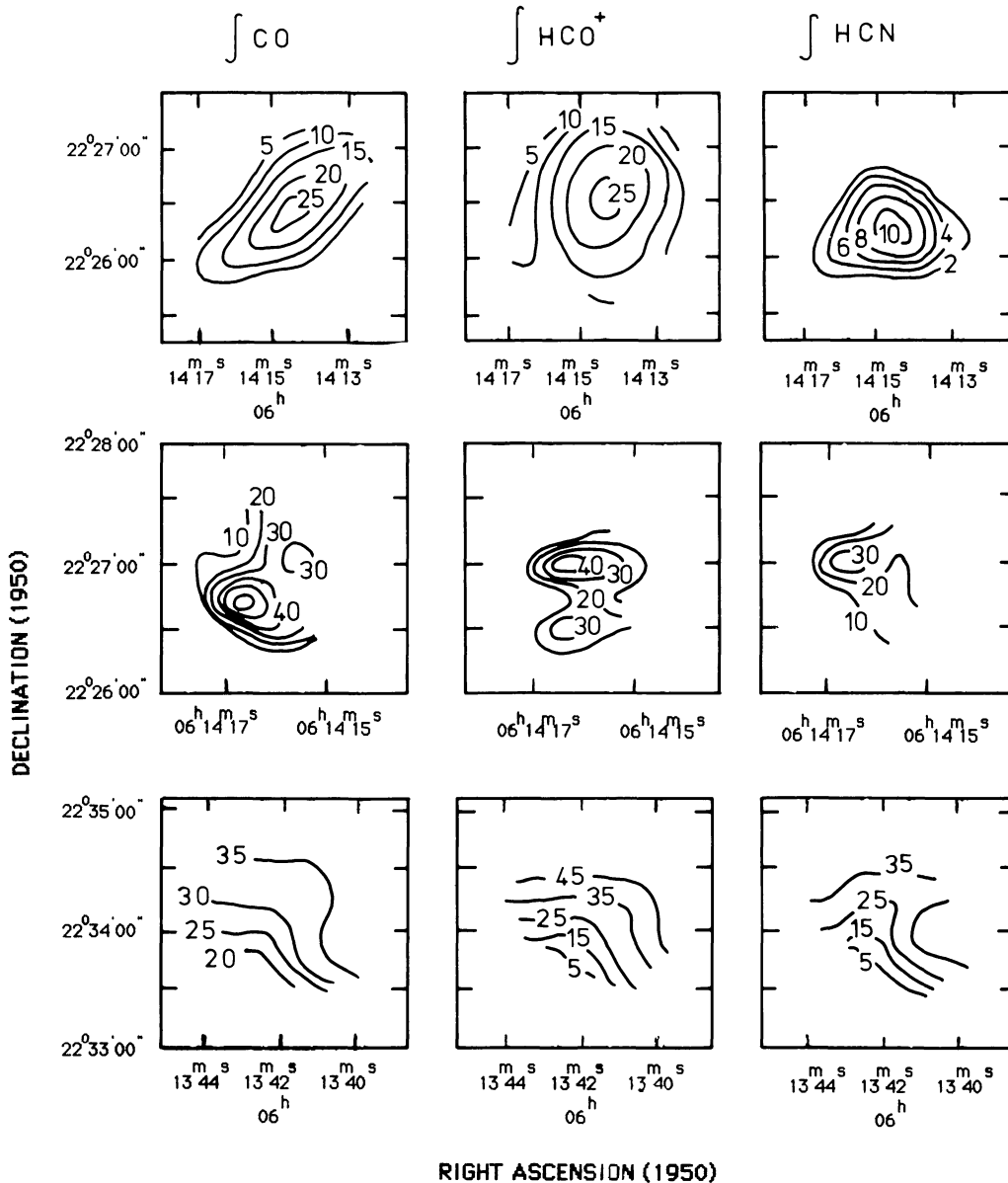
Fig. 5. Maps of the distribution of T_A^* for CO, HCN and HCO$^+$ for some other areas in IC 443, integrated from -90 to $0\,\mathrm{km\,s^{-1}}$. The contours are in annotated on the individual maps in $\mathrm{K\,km\,s^{-1}}$

positions IC 443B and C, after we have convolved the $J = 1 - 0$ data to synthesize the larger $J = 3 - 2$ beam. This *qualitatively* supports the trend seen in the $J = 2 - 1$ data at other positions.

3.2. Molecular line survey

We have carried out a molecular line survey in several frequency ranges between 84 and 115 GHz using the Nobeyama telescope. This survey has included the frequencies of 13 transitions chosen as useful diagnostics of the evolution of the chemical abundances in a cloud which has been subject to the passage of an interstellar shock. The chemistry of shocked regions has been discussed by many authors, whose work has been summarised by Mitchell (1984) and Dalgarno (1985) and references therein. For these models, specific predictions can be made for the variation

of molecular abundances as functions of time, density and shock parameters. Mitchell and Deveau (1983) have discussed the consequences of the passage of a $10\,\mathrm{km\,s^{-1}}$ shock through a $100\,\mathrm{cm^{-3}}$ density cloud, and subsequently Mitchell (1984) carried out a similar calculation for a higher density cloud with $n(\mathrm{H_2})$ of $10^4\,\mathrm{cm^{-3}}$. In Table 1, the details of the present molecular line survey are listed for the two positions in the shocked regions which we studied.

The first position at RA (1950) = $06^h14^m41\overset{s}{.}9$, DEC (1950) = $+22°22'40''$, was the centre of the highest velocity shocked gas; the second at RA (1950) = $06^h14^m44\overset{s}{.}1$, DEC (1950) = $+22°23'30''$, was selected as having intense, but with only moderate velocity gas ($\Delta v = 18\,\mathrm{km\,s^{-1}}$) present. The detected lines show some variation in line intensity; HCN being more intense at the higher velocity position, HCO$^+$ and CS having a similar intensity at both positions. The CS line detections are shown in Fig. 9.
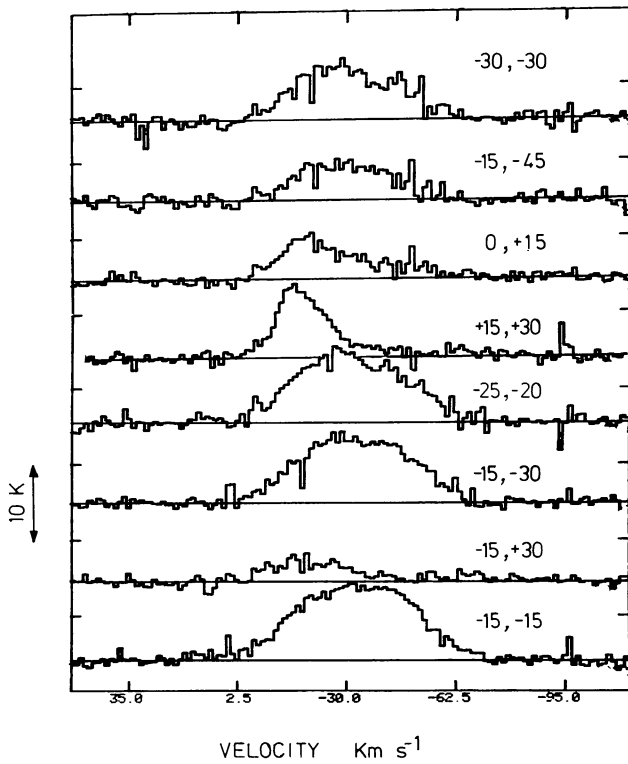
Fig. 6. Spectra obtained in the CO J=2−1 transition towards several positions near the SE rim. The vertical axis is in units of main beam brightness temperature K. The offsets indicated on the figures are in arc seconds relative to the reference position at RA (1950) = 06^{h}14^{m}43^{s}0, DEC (1950) = +22°23′00″
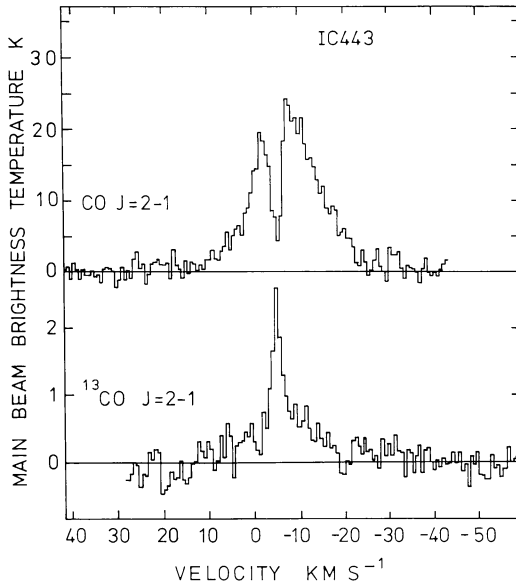
Fig. 7a. J=2−1 CO and ^{13}CO spectra towards the position RA (1950) = 06^{h}13^{m}42^{s}0, DEC (1950) = +22°33′40″, obtained with the Kitt Peak 12 m telescope

In Table 2, we have estimated, for the *optically thin case*, the relative molecular abundances (or upper limits) for the lines included in the survey. These have been summarised according to the transition giving the most stringent limit, or the most ac-
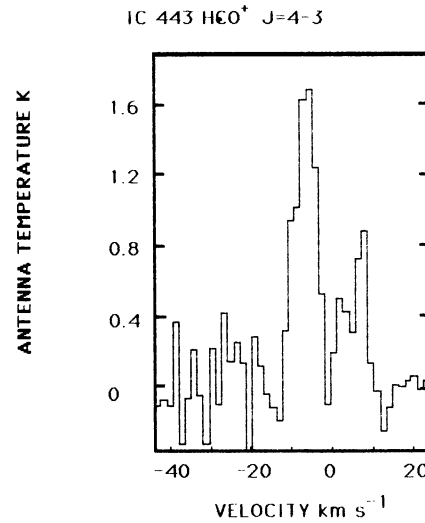

Fig. 7b. HCO$^+$ J=4−3 spectrum towards the same position as Fig. 7a obtained at the UKIRT 3.8 m telescope. For this spectrum, the vertical scale is in units of corrected antenna temperature T_r^* K

curate detection. We have used the following relationship for simple linear molecules

$$N_{col} = \frac{c_1 \int T_R \, dv \exp\left(\frac{c_2 J(J+1)B}{T}\right)}{B\tilde{\mu}^2(J+1)\left(1 - \exp\left(\frac{2c_2(J+1)B}{T}\right)\right)} \qquad (1)$$

where $\int T_r \, dv$ is the integrated intensity of the line, N_{col} is a lower limit on the column density, B is the rotational constant, T the excitation temperature on the ladder of energy levels, and the constants C1 = 1.6 10^{14} and C2 = 4.8 10^{-2}. This equation has a dependence on excitation temperature, and assumes that it is the same for all transitions of a molecule. Since we do not know the value of the excitation temperature, we have chosen to calculate the ratio $n(X)/n(CO)$, thus removing to first order, the temperature dependence. Assuming that all of the molecular species are excited in the same volume of gas as the CO, we then adopt an abundance ratio of $X(CO) = 5\,10^{-5}$, and hence deduce the relative molecular abundances listed. We point out that this approximation, adopted by DeNoyer and Frerking (1981) and Dickinson et al. (1980), is valid only for conditions where the optical depth is much less than unity, and $T_{ex} = T_{kin}$. As we will show later, these conditions may not be satisfied for all of the lines studied, and results derived using this approximation should be treated with caution. For more complex non-linear molecular species, the expression

$$N_1 = \frac{8\pi v^3}{TA_{ul}c^3} \frac{g_1}{g_u} \frac{1}{(1 - \exp(-hv/kT))} \qquad (2)$$

should be used, where N_1 is the total column density of molecules in the lower level, g_u and g_1 are the statistical weights for the upper and lower levels respectively, and A_{ul} is the Einstein coefficient. To get from N_1 to the total column density of the molecular species, N_{col}, the expression

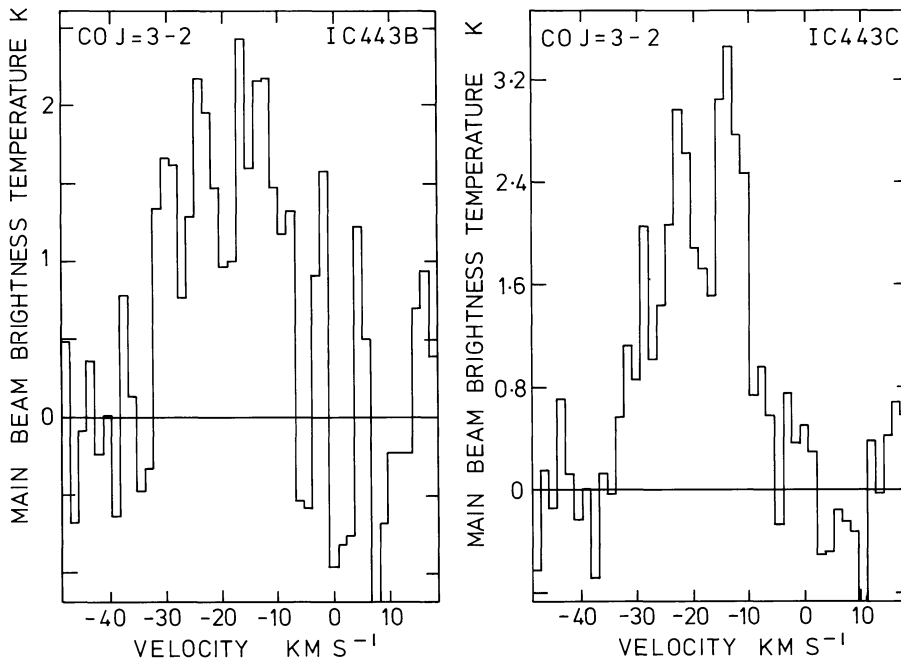$$N_{col} = \frac{N_1 Q(T)}{g_1 \exp(-E_1/kT)} \qquad (3)$$

Fig. 8. CO J=3−2 spectra obtained at UKIRT towards the positions IC 443B and IC 443C (following the nomenclature of DeNoyer, 1979), in the SE rim of the supernova remnant shell

is used, where E_l is the energy above the ground state, and $Q(T)$ is the partition function.

The temperature structure of the postshock zone is complex, and it is likely that a whole range of gas temperatures may be present (Hollenbach and McKee, 1979; Phillips and White, 1981;

Mitchell, 1984). For non-dissociative shocks, the cooling time is quite rapid, and the postshock temperatures will probably fall below 50 K in about 30 years. The case of a dissociative shock is rather different, and in the absence of major molecular coolants (which are destroyed by the shock), the postshock gas cools much

Table 1

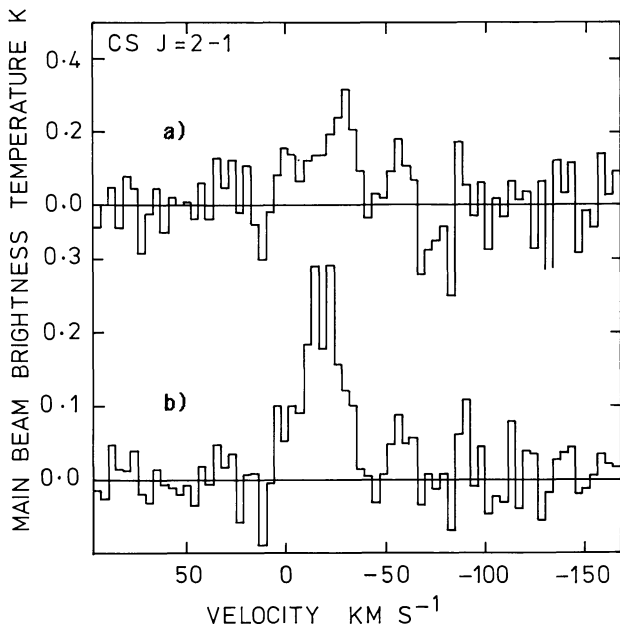| Species	Frequency (MHz)	Intensity T_r^* K	
		RA: $06^h14^m41^s9$ DEC: $+22°22'40''$ v_{lsr}: $-30\,km\,s^{-1}$	$06^h14^m44^s1$ $+22°23'30''$ $-16\,km\,s^{-1}$
CH_3OH	84423	<0.10	<0.08
OCS	85139		
HCS^+	85347	<0.12	<0.17
SO	86093	<0.12	<0.15
SiO $v=1$	86243	<0.12	<0.15
$H^{13}CN$	86340	<0.12	<0.15
CH_3OH	86615	<0.10	<0.10
SO_2	86639	<0.12	<0.12
$H^{13}CO^+$	86754	<0.08	<0.08
SO_2	86828	<0.16	<0.16
SiO $v=0$	86846	<0.16	<0.16
CH_3OH	86903	<0.12	<0.12
HCN	88631	0.81	<0.25
HCO^+	89188	1.9	1.9
SO_2	97702	<0.17	<0.17
CS	97981	0.27	0.23
H_2CS	104616	<0.11	<0.09
CO	115271	4.5	6.5
^{13}CO	220399	≤0.2	
CO	230538	6.2	6.4
CO	34596		1.7

Fig. 9a and b. CS $J = 2-1$ detections in the SE rim of IC 443 at the positions (1950 coordinates RA, DEC): **a** $06^h14^m41^s9$, $+22^h22'40''$; **b** $06^h14^m44^s1$, $+22°23'30''$

more slowly in a thin layer behind the shock (Phillips and White, 1981). The optical study by Fesen and Kirshner (1980) suggests that the shock velocity is 65–100 km s^{-1}. On the basis of these studies, and in the absence of knowledge of the true kinetic or excitation temperatures in the region for the size scales we have measured, we have chosen to model the data using values of 50 and 100 K for the kinetic temperature of the shock excited gas. These values have been selected to enable us to make *first order* estimates of molecular densities and abundances in the cases of hot gas, and for a cooler, perhaps compressed, gas. We are unable to determine whether the shock in IC 443 does actually lead to dissociation of the molecular material, despite the very high velocities observed. This uncertainty depends on the ability of magnetic fields to soften the shock in IC 443 sufficiently to pre-

vent dissociation occurring, and our lack of knowledge as to how the magnetic softening process operates.

The evidence from the CO and ^{13}CO data of DeNoyer (1979) and also this work, suggest that the high velocity CO is optically thin. We have applied the LVG approximation (Goldreich and Kwan, 1974; see also Draine and Roberge, 1984) to obtain a first order estimate of the excitation conditions in the emitting gas, from the observed intensities of the CO lines. After correcting for the relative efficiencies of the various telescopes, we find the best fit for the high velocity emitting fragment at RA (1950) = $06^h14^m41^s9$, DEC (1950) = $+22°22'40''$, is (the first numbers quoted from now on refer to $T_{kin} = 100$ K, the second number, given in brackets, is for $T_{kin} = 50$ K) $n(H_2) = 2000(3500)$ cm^{-3}, and the molecular abundance per unit velocity gradient, $X/(dV/dR) = 8\,10^{-7}$ $(5\,10^{-7})$ km^{-1} s pc. Since this estimate is dependent on the accuracy of the calibration procedure used to derive main beam brightness temperatures, we have examined the resultant uncertainty in the LVG solution based on conservative estimates of any calibration errors. We believe that the results of the LVG calculation are good to within a factor of 2–3 in both density and molecular abundance per unit velocity gradient. In order to calculate X(CO), we have estimated the deconvolved diameter of the high velocity emitting cloud to be $4.5\,10^{17}$ cm (for a distance of 1.5 kpc estimated by Fesen and Kirshner, 1980). Assuming the linewidth to represent the velocity spread over the fragment, we then estimate $dV/dR = 275$ km s^{-1} pc^{-1}. Thus we deduce the CO abundance relative to H_2, X(CO), is $2.2\,10^{-4}$ $(1.4\,10^{-4})$. This is approximately 4 times greater than the commonly assumed value for galactic molecular clouds. At the position RA (1950) = $06^h13^m42^s0$, DEC (1950) = $+22°33'40''$, the best fit from our LVG modelling is $n(H_2) = 1800\,(8000)$ cm^{-3} and $X/(dV/dR) = 2.5\,10^{-6}$ $(1.2\,10^{-6})$. For lower assumed temperatures, the derived density will be slightly higher, and the abundance lower. Similarly for this position we estimate $dV/dR = 75$ km s^{-1} pc^{-1}, and X(CO) = $1.9\,10^{-4}$ $(9\,10^{-5})$. It remains unclear whether the difference between the values for relative abundance estimated at these two positions, and the commonly accepted value, is real, or a consequence of the assumptions of the LVG analysis we have carried out. A very large abundance increase for CO is not expected on the basis of shock chemistry models, since none of the formation routes to CO in the recombining gas behind a dissociative shock contain a strong temperature dependence (Mitchell and Deveau, 1983), although these models do predict a small abundance increase relative to an unshocked cloud.

In the example of this latter solution, the excitation temperature of the CO $J = 2-1$ transition is 24 (20) K, and the optical depth is 2.7 (1.7). The maximum CO optical depth, 2.4 (2.2), occurs in the CO $J = 3-2$ transition. For this example the observed ^{13}CO $J = 2-1$ data are well matched by an isotopic ratio CO/^{13}CO = 89, and we can exclude any value for the isotopic abundance ratio less than 70. We then use the LVG estimate for this position to indicate that any beam dilution, due for example to clumping, is small, and that most probably the emitting material is not significantly clumped on size scales smaller than that corresponding to our beam size.

Assuming that HCO$^+$ and HCN are excited in the same volume of gas as the CO, as seems likely from the similar spatial distributions and spectral profiles, the LVG approximation can be used to estimate the excitation of this gas, and compare it with the relative abundances given in Table 2 for the optically thin

Table 2

Species	Position	
	RA: $06^h14^m41^s9$ DEC: $+22°22'40''$	$06^h14^m44^s1$ $+22°23'30''$
	Molecular Abundance	
CO	assume $5\,10^{-5}$	assume $5\,10^{-5}$
HCS$^+$	$<4.7\,10^{-9}$	$<9.9\,10^{-9}$
SO	$<1.1\,10^{-8}$	$<1.3\,10^{-8}$
SiO	$<3.0\,10^{-9}$	$<3.2\,10^{-9}$
SO$_2$	$<1.5\,10^{-7}$	$<1.5\,10^{-7}$
HCN	$<4.4\,10^{-9}$	$2.2\,10^{-8}$
HCO$^+$	$4.1\,10^{-8}$	$4.1\,10^{-8}$
CH$_3$OH	$<3.5\,10^{-7}$	$<4.5\,10^{-7}$
H$_2$CS	$<4.0\,10^{-9}$	$<7.2\,10^{-9}$
CS	$3.4\,10^{-9}$	$1.9\,10^{-9}$

approximation. For the HCO⁺ and HCN $J=1-0$ transitions, $X/(dV/dR) = 1.6\,10^{-8}\,(1.2\,10^{-9})$ and $3.2\,10^{-8}\,(4\,10^{-9})\,km^{-1}\,s\,pc$ respectively at the RA (1950) = 06^{h}13^{m}42^{s}0, DEC (1950) = +22°33′40″ position. Similarly at RA (1950) = 06^{h}14^{m}41^{s}9, DEC (1950) = +22°22′40″ we estimate $X/(dV/dR) = 6.3\,10^{-9}$ $(1.6\,10^{-9})$ and $4\,10^{-9}\,(2.5\,10^{-9})\,km^{-1}\,s\,pc$. Assuming the values for dV/dR adopted previously, we then estimate $X(HCO^+) = 1.7\,10^{-6}\,(4.4\,10^{-7})$ and $1.2\,10^{-6}\,(1\,10^{-7})$, and $X(HCN) = 1.1\,10^{-6}$ $(7\,10^{-7})$ and $2.4\,10^{-6}\,(3\,10^{-7})$, for the RA (1950) = 06^{h}14^{m}41^{s}9, DEC (1950) = +22°22′40″ and RA (1950) = 06^{h}13^{m}42^{s}0, DEC (1950) = +22°33′40″ positions respectively. These values differ somewhat from those calculated on the basis of the optically thin assumption used in Table 2. From the LVG calculation we find the assumption of optical thinness to be incorrect. The LVG estimate of the optical depths of HCO⁺ and HCN are 10–15, and the excitation temperatures are 3–6 K in the $J=1-0$ lines for $T_{kin} = 100$ K. This indicates that the transitions are both optically thick and sub-thermally excited. This may explain the reason why at some positions, the CO linewidth is less than that of HCO⁺, as we have remarked in an earlier section.

The ratios of $X(HCO^+)/X(HCN)$ observed in IC 443 lie in the range 0.6–2, consistent with the values determined by Wootten et al. (1978) for galactic clouds. However, the abundances of *both* species relative to CO are 2–3 orders of magnitude *greater* than those seen towards the Wootten et al. (1978) sample of higher density ($n(H_2) = 10^4$–10^6 cm^{-3}) cloud cores. The dependence of the relative abundances of CO, HCN and HCO⁺ with cloud density and properties have been discussed in some detail by Wootten et al (1978) and Wootten et al. (1980). We note that the abundances of HCN and HCO⁺ determined here, are similar to those predicted in the shock chemistry calculations for an unshielded cloud, of Mitchell and Deveau (1983), at a time corresponding to 100–200 years after the passage of a 10 km s^{-1} shock, although this velocity is almost an order of magnitude less than the expansion velocity of the supernova remnant.

In a similar way, we have used the LVG model for the CS $J=2-1$ line observed at the RA (1950) = 06^{h}14^{m}41^{s}9, DEC (1950) = +22°22′40″ position, to examine its excitation. Assuming CS to be excited in the same volume of gas as the CO, HCO⁺ and HCN, we find $X(CS) = 7\,10^{-7}$ for $T_{kin} = 100$ K, the optical depth is approximately 2, and the excitation temperature is less than 5 K. The abundance estimate is again somewhat higher than for the optically thin case, and agrees well with the prediction for $X(CS)$ in the Mitchell and Deveau (1983) model. If we assume, based on the HCN, HCO⁺ and CS measurements, that the chemistry of the region is consistent with the passage of a shock during the past few hundred years, then we note with interest that the CO abundance is also predicted to increase by a small amount, and is within a factor of two of that estimated from our LVG modelling of these two positions.

4. Discussion

The present data, coupled with the shocked molecular hydrogen observations of Burton et al (private communication), show clear evidence for interaction of a shock associated with the expanding shell of IC 443, and a nearby molecular cloud. Such interactions may not be unique to IC 443, and it is possible that Mon OB1/2, CMa OB1 (Blitz, 1978), W28 and W44 (Wootten, 1977, 1981; DeNoyer, 1983) and several other supernovae (Braun and Strom

preprint) may show some similar (although less violent) interaction with nearby molecular clouds.

The effects of the passage of the shock in IC 443 are quite clear, strong excitation of the neutral (and ionised) molecular material has occurred (and probably still is occurring). This has led to substantial fragmentation of the molecular cloud material on size scales of several tenths of a parsec, and there are suggestions that the individual cloud fragments may have been imparted with velocities relative to each other of up to 10–20 km s^{-1}.

Such fragmentation is expected after a strong shock has been incident on a cloud of neutral material (see for example McKee et al., 1984, and references therein). A strong shock (>55 km s^{-1}) will dissociate the hydrogen, and in the postshock radiative zone where the hydrogen will recombine, Rayleigh-Taylor instabilities can lead to extensive fragmentation (McKee and Hollenbach, 1983; Vishniac, 1983). The present observations support the existence of such fragmentation. Assuming the average density in the fragments is about 1500 cm^{-3}, we then estimate their masses to be typically 0.1–0.3 solar masses. These are substantially less than will be needed for subsequent collapse to a star, and it is likely that if star formation is to occur in these fragments, the individual clumps will need to coalesce. However, as can be seen from Fig. 3, the shock has imparted considerable individual velocities to some of the fragments, and the system as a whole is dynamically unstable. It is probable that the fragments will disperse rather than coagulate, and therefore shock induced star-formation is not likely to result.

The observed abundance enhancements for HCO⁺, HCN and CS reported here, provide support for shock chemistry modelling such as that of Mitchell and Deveau (1983, and references therein). Calculation of the relative molecular abundances is clearly difficult to do in a unique way, the particular choice of the two models used here showing an extreme example of the inherent problems. It is likely that the LVG technique used here is more realistic than the analytically simpler treatment adopted by DeNoyer and Frerking (1981), but undoubtedly a more complex treatment of the radiative transfer which incorporates the effects of turbulence and fragmentation will eventually need to be developed.

5. Conclusions

1. Several areas of shocked molecular material have been mapped in the CO, HCN and HCO⁺ $J=1-0$ transitions. The spatial structure of the emitting regions consists of a number of small (diameter 0.1–0.3 pc) fragments of molecular material, whose spectral shapes are characterised by wide linewidths. The spatial distributions of all three molecular species are very similar, and are strongly correlated with the distribution of shocked molecular hydrogen.

2. For two of the fragments, we have used LVG modelling techniques to estimate the densities and molecular abundances. From a comparison of CO and ^{13}CO measurements in the CO $J=1-0$ and $2-1$ transitions, we find $n(H_2) = 1500$–2000 cm^{-3} and $X(CO) = 2\,10^{-4}$.

3. A survey in a number of molecular species chosen as potential indicators of the effects of shocks on the molecular abundances in a cloud has been carried out. The abundances of HCN, HCO⁺ and CS are enhanced relative to those more typical of dense molecular cloud cores. The $J=1-0$ transitions HCN,

HCO$^+$ and CS are found to be optically thick and subthermally excited. In consequence, previous estimates of molecular abundances (or upper limits) in the shocked gas of IC 443 may be in error. The inferred molecular abundances are in good agreement with those predicted in shock chemistry calculations, assuming that the shock has interacted with the cloud very recently. We find the high velocity CO emission to be optically thin in the $J = 1 - 0$ transition, but becoming optically thick in the $J = 2 - 1$ and $3 - 2$ transitions. The data are consistent with an isotopic abundance ratio, C/^{13}C, greater than 70.

4. The structure of the cloud is consistent with its fragmentation into a number of clumps with masses 0.1–0.3 solar masses. As a system, the clumps are dynamically unstable, and are unlikely to form stars.

References

Blitz, L.: 1978, Ph.D. Thesis, Columbia University
Burton, M.: 1986, (private communication)
Cornett, R.H., Chin, G., Knapp, G.R.: 1977, *Astron. Astrophys.* **54**, 889
Dalgarno, A.: 1985, preprint of talk at Bad Wisconsin conference
DeNoyer, L.K.: 1978, *Monthly Notices Roy. Astron. Soc.* **183**, 187
DeNoyer, L.K.: 1979, *Astrophys. J.* **232**, L165
DeNoyer, L.K., Frerking, M.A.: 1981, *Astrophys. J.* **246**, L37
DeNoyer, L.K.: 1983, *Astrophys. J.* **264**, 141
Dickinson, D.F., Rodriguez-Kuiper, E.N., St. Clair Dinger, A., Kuiper, T.B.H.: 1980, *Astrophys. J.* **237**, L43
Draine, B.T., Roberge, W.G.: *Astrophys. J.* **282**, 491
Fesen, R.A., Kirshner, R.P.: 1980, *Astrophys. J.* **242**, 1023
Goldreich, P, Kwan, J.: *Astrophys. J.* **189**, 441
Hollenbach, D.J., McKee, C.F.: 1979, *Astrophys. J. Suppl.* **41**, 555
Huang, Y-L., Dickman, R.L. and Snell, R.L.: 1986, *Astrophys. J. Letters* **302**, L63
McKee, C.F., Chernoff, D.F. Hollenbach, D.J.: 1984, *Galactic and Extragalactic Infrared Spectroscopy*, D. Reidel Press, p. 103
Mitchell, G.F.: 1984, *Astrophys. J. Suppl.* **54**, 81
Mitchell, G.F. and Deveau, T.J.: 1983, *Astrophys. J.* **266**, 646
Phillips, J.P., and White, G.J.: 1981, *Monthly Notices Roy. Astron. Soc.* **194**, 15
Treffers, R.B.: 1979, *Astrophys J.* **233**, L17
Vishniac, E.T.: *Astrophys. J.* **274**, 152
White, G.J., Phillips, J.P., Watt, G.D.: 1981, *Monthly Notices Roy. Astron. Soc.* **197**, 745
White, G.J., Monteiro, T.S., Richardson, K.J., Griffin, M.J., Rainey, R.: 1986, *Astron. Astrophys.* **162**, 253
Wootten, H.A.: 1977, *Astrophys. J.* **216**, 440
Wootten, H.A.: 1981, *Astrophys. J.* **245**, 105
Wootten, H.A., Evans, N.J., Snell, R. Vanden Bout, P.: 1978, *Astrophys. J.* **225**, L143
Wootten, H.A., Snell, R., Evans, N.J.: 1980, *Astrophys. J.* **240**, 532